Hemispherical total emissivity and specific heat capacity of deeply undercooled $Zr_{41.2}Ti_{13.8}Cu_{12.5}Ni_{10.0}Be_{22.5}$ melts

R. Busch,[a] Y. J. Kim, and W. L. Johnson
W. M. Keck Laboratory of Engineering Materials, California Institute of Technology, Pasadena, California 91125

A. J. Rulison[b] and W. K. Rhim
Jet Propulsion Laboratory, California Institute of Technology, Pasadena, California 91109

D. Isheim
Institut für Metallphysik der Universität Göttingen, Hospitalstrasse 3-7, 37073 Göttingen, Germany

(Received 20 December 1994; accepted for publication 13 March 1995)

High-temperature high-vacuum electrostatic levitation (HTHVESL) and differential scanning calorimetry (DSC) were combined to determine the hemispherical total emissivity ϵ_T, and the specific heat capacity c_p, of the undercooled liquid and throughout the glass transition of the $Zr_{41.2}Ti_{13.8}Cu_{12.5}Ni_{10.0}Be_{22.5}$ bulk metallic glass forming alloy. The ratio of c_p/ϵ_T as a function of undercooling was determining from radiative cooling curves measured in the HTHVESL. Using specific heat capacity data obtained by DSC investigations close to the glass transition and above the melting point, ϵ_T and c_p were separated and the specific heat capacity of the whole undercooled liquid region was determined. Furthermore, the hemispherical total emissivity of the liquid was found to be about 0.22 at 980 K. On undercooling the liquid, the emissivity decreases to approximately 0.18 at about 670 K, where the undercooled liquid starts to freeze to a glass. No significant changes of the emissivity are observed as the alloy undergoes the glass transition.

The hemispherical total emissivity ϵ_T, which is the ratio of energy emitted by a material at a temperature T with respect to a blackbody at the same temperature, has been measured for several solid metals,[1–4] alloys,[5] and semiconductors.[6] However, there is a lack of emissivity data on liquid metals and only recently first results were reported for undercooled metallic liquids.[7] Lately, new multicomponent alloy systems have been found such as La–Al–Ni,[8] Zr–Al–Cu–Ni,[9] and Zr–Ti–Cu–Ni–Be[10] exhibiting an extraordinary thermal stability of the undercooled liquid with respect to crystallization. Cooling rates of less than 100 K/s are usually sufficient to suppress nucleation of crystalline compounds and thus form a bulk metallic glass in these alloy systems. For the particular $Zr_{41.2}Ti_{13.8}Cu_{12.5}Ni_{10.0}Be_{22.5}$ alloy we even showed that the melt could be undercooled more than 350 K below the liquidus temperature, $T_{liq}=993$ K, applying cooling rates lower than 2 K/s. The melt then undergoes the glass transition.[11] This deep undercooling of a liquid alloy melt without crystallization was achieved in a high-temperature high-vacuum electrostatic levitator (HTHVESL). It offers the opportunity to investigate thermophysical properties of undercooled metallic melts in regions which have not been accessible so far. In this letter the hemispherical total emissivity ϵ_T, and the specific heat capacity c_p, of the $Zr_{41.2}Ti_{13.8}Cu_{12.5}Ni_{10.0}Be_{22.5}$ alloy are determined in the undercooled liquid state as well as in the glass transition region by measuring c_p/ϵ_T as a function of temperature in the HTHVESL and combining the data with specific heat capacity measurements in a differential scanning calorimeter (DSC).

Amorphous alloy ingots with a composition $Zr_{41.2}Ti_{13.8}Cu_{12.5}Ni_{10.0}Be_{22.5}$ were prepared from a mixture of the elements by induction melting. Pieces of typically 40 mg were remelted in a radio frequency field to produce spherical specimens.

All HTHVESL experiments were performed under ultrahigh vacuum conditions ($P<7\times10^{-3}$ mPa). The details of the experimental apparatus are described elsewhere.[12] The main feature and advantage of the HTHVESL compared to electromagnetic levitation is that levitation and heating of the sample are decoupled, so that the sample can be cooled from above the melting point down to room temperature and kept levitated at the same time without significant energy input. Specific heat capacities of the glass, the undercooled liquid, and the crystalline state were measured using a Perkin Elmer DSC7. The continuous change in c_p on heating the glass or cooling the undercooled liquid was measured in both heating and cooling experiments for different rates of temperature change. In addition, the absolute values of c_p in the amorphous alloys up to 593 K and in the crystallized samples up to 893 K were determined in reference to a sapphire standard. Details on the DSC experiments can be found elsewhere.[13]

Figure 1 presents a typical cooling curve for a spherical sample of the $Zr_{41.2}Ti_{13.8}Cu_{12.5}Ni_{10.0}Be_{22.5}$ alloy obtained in the HTHVESL after removing the heat source. Due to the unique design of the HTHVESL the heat transfer resulting from conductive and convective cooling in a gas, and any heat input Q_{in} from an external source can be neglected, in

[a]Electronic mail: busch@hyperfine.caltech.edu
[b]Now at the Dept. of Chemical Engineering, John Hopkins University, Baltimore, MD 21218.

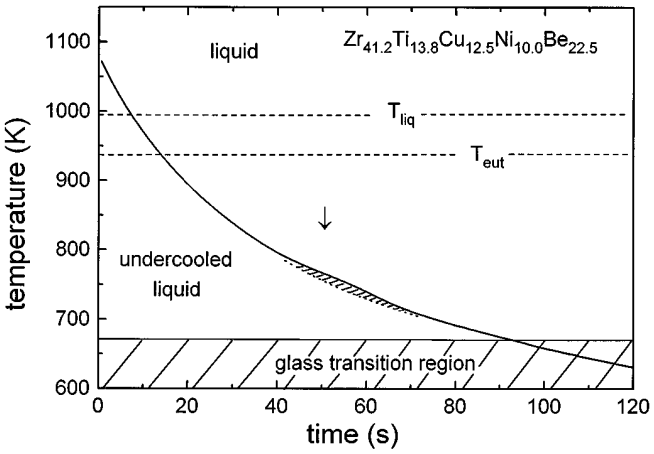

FIG. 1. Temperature–time profile of a $Zr_{41.2}Ti_{13.8}Cu_{12.5}Ni_{10.0}Be_{22.5}$ sample alloy, which is undercooled below the liquidus temperature T_{liq}, and eutectic temperature T_{eut}. The undercooled liquid freezes to a glass in the glass transition region (hatched). A small exothermic effect is observed at about 750 K (arrow).

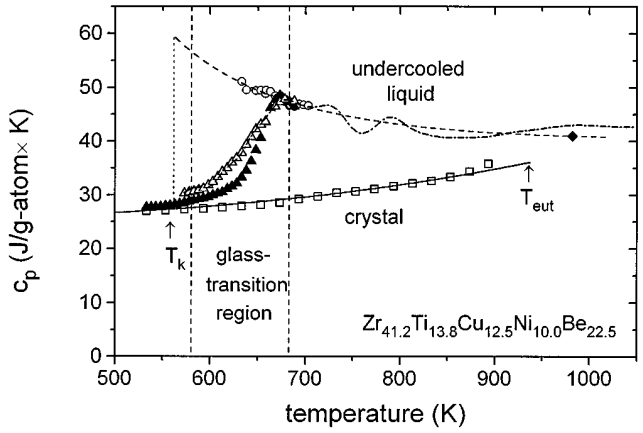

FIG. 3. Specific heat capacity of the undercooled liquid (○◆), throughout the glass transition on heating (▲) and cooling (△) with 1.67 K/s, and of the crystal (□), measured with a DSC. The specific heat capacity curve determined by the $c_p/\epsilon_T(T)$ curve is plotted as a dashed–dotted line. Additionally, drawn is a fit to the specific heat capacity data of the undercooled liquid according to a $1/T^2$ law (dashed) (Ref. 13).

contrast to electromagnetic levitation (see also Ref. 14). Hence, the cooling process is purely radiative and determined by the following heat balance equation

$$mc_p(T)\frac{dT}{dt} = -\epsilon_T(T)A\sigma(T^4 - T_s^4), \tag{1}$$

where m is the mass of the sample with a surface area A, T is the temperature of the sample, T_S is the temperature of the surroundings, and σ is the Stephan–Boltzmann constant. Since the cooling curve $T(t)$ of the spherical sample with a known mass and density is only a function of c_p and ϵ_T, the ratio c_p/ϵ_T as a function of temperature can be determined from the shape of the cooling curve.[7] The density of the liquid sample is assumed to be constant. Figure 2 shows the c_p/ϵ_T curve obtained by averaging 14 different cooling curves. The uncertainty of the calculated c_p/ϵ_T values is ± 20 J/g-atom K at any given temperature. Figure 2 indicates that c_p/ϵ_T rises with increasing undercooling and starts to drop at about 670 K. This temperature is the beginning of the glass transition for cooling at the present cooling rate, as determined by DSC experiments. At about 750 K an anomaly in the c_p/ϵ_T curve is observed. It is due to a very small recalesence effect, that is barely visible in each cooling curve (see Fig. 1) representing a small heat release. This exothermic effect can be either due to nucleation of crystalline compounds or to the beginning of a decomposition reaction of the alloy in the undercooled liquid state. Based on x-ray diffraction and DSC experiments, comparing the sample processed in the levitator with an amorphous reference sample, we showed that the upper limit for crystalline parts in the sample is less than 2%.[11] This favors the latter explanation. Decomposition in the amorphous or undercooled liquid state was also found in the La–Al–Ni[15] system and even appears in binary metallic glasses where different short range orders can develop depending on composition.[16] In addition, if the decomposition proceeds via a spinodal unmixing process it can be favored compared to nucleation of crystalline compounds as there is no nucleation barrier to overcome.[17]

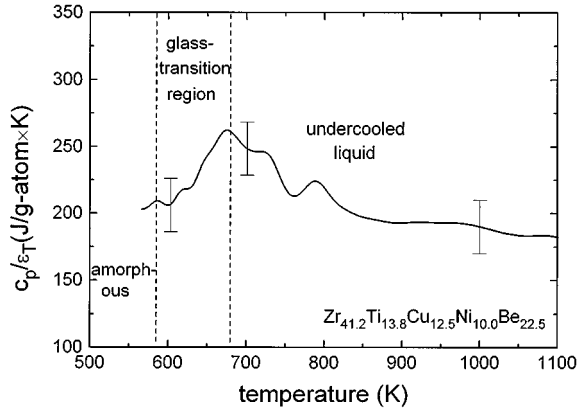

FIG. 2. The measured ratio c_p/ϵ_T as a function of temperature during radiative cooling. c_p/ϵ_T rises with decreasing temperature and to drops as soon as the undercooled liquid starts to freeze to a glass. The anomaly observed at 750 K reflects the small recalesence effect observed in the cooling curve.

ϵ_T is evaluated using data obtained by the DSC experiments.[13] In Figure 3 the measured specific heat capacities are displayed. Specific heat capacities of the metastable undercooled liquid are marked as circles. These data were obtained by measuring the track of c_p the from the amorphous alloy throughout the glass transition into the undercooled liquid with different heating rates between 0.0167 and 6.67 K/s.[13] The specific heat capacity of the liquid above the eutectic temperature is marked as a diamond.[18] The dashed curve represents the specific heat capacity of the undercooled liquid fitted to the experimental data according to a $1/T^2$ law.[13,19] The curve is extrapolated down to the Kauzmann temperature T_K, which represents the lower bound for the glass transition for thermodynamical reasons (see Ref. 13). However, the c_p values of the undercooled liquid below about 620 K are only accessible for heating and cooling rates below 0.0167 K/s. In contrast, the cooling rates in the HTH-VESL experiment are of the order of 2 K/s. For this cooling rate the undercooled liquid falls out of metastable equilib-

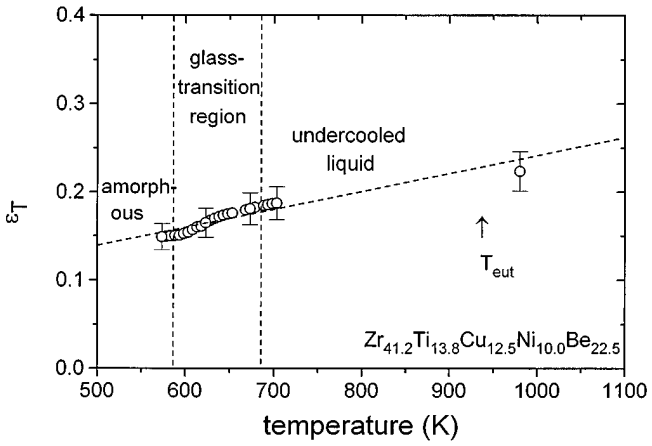

FIG. 4. Hemispherical total emissivity of the $Zr_{41.2}Ti_{13.8}Cu_{12.5}Ni_{10.0}Be_{22.5}$ alloy in the undercooled liquid and throughout the glass transition.

rium far above the Kauzmann temperature and c_p starts to drop. This is shown in Fig. 3 as well. The open triangles in Fig. 3 show the track of c_p of a sample cooled in the DSC with a rate of 1.667 K/s throughout the glass transition. The curve starts to deviate from the specific heat capacity curve of the undercooled liquid below about 670 K, that corresponds to the temperature below which c_p/ϵ_T measured in the HTHVESL starts to drop as well.

Taking the c_p/ϵ_T data from Fig. 2, the hemispherical total emissivity is calculated for each measured c_p value. Below 670 K the c_p data of the sample cooled in the DSC with 1.67 K/s are used. The resulting ϵ_T as a function of temperature is shown in Fig. 4. Due to the lack of direct c_p measurements between 710 and 980 K, the emissivity is interpolated as a straight line. This is most likely a good approximation since, in general, there is a virtually linear relationship between the electrical resistivity and the hemispherical total emissivity for pure metals.[4] Furthermore, the temperature dependence of the resistivity in liquid metals and alloys is weak and linear as well.[20] As can be observed in Fig. 4, the emissivity of the melt is 0.22 at 980 K and decreases to a value of 0.18 in the deeply undercooled melt just above the glass transition. When the sample starts to freeze to a glass at about 670 K no significant change of ϵ_T is observed within the experimental error. This is in good agreement with results of Geyer,[21] who showed that the dc resistivity of the amorphous $Zr_{41.2}Ti_{13.8}Cu_{12.5}Ni_{10.0}Be_{22.5}$ alloy changes only slightly as the alloy is heated above the glass transition.

In contrast to solidification by crystallization, significant changes in the surface morphology that affect the emittance do not appear during solidification by freezing the undercooled $Zr_{41.2}Ti_{13.8}Cu_{12.5}Ni_{10.0}Be_{22.5}$ liquid to a glass. It was shown by atomic force microscopy,[22] that the free surfaces of the amorphous $Zr_{41.2}Ti_{13.8}Cu_{12.5}Ni_{10.0}Be_{22.5}$ alloys exhibit an extraordinary smoothness of ± 5 nm on a typical length scale of more than 1 μm. So we assume that artifacts produced by a change of the surface morphology can be neglected in this particular case.

The emissivity data as a function of temperature were used to determine the specific heat capacity of the undercooled liquid by multiplying them with the c_p/ϵ_T curve. The calculated c_p from the undercooling experiment is added in Fig. 3 (dashed–dotted line). The c_p data throughout the glass transition fits the experimental data obtained in the DSC on cooling, since those were used to calculate the emissivity. For the undercooled liquid region the c_p obtained from the levitation experiments is in good agreement with the $1/T^2$ law (dashed) until the metastable undercooled melt falls out of metastable equilibrium at 670 K and starts to undergo the glass transition. Only at 750 K, where a weak recalesence effect occurred, as discussed above, the deviations are larger.

In this letter we described an experimental approach to determine the hemispherical total emissivity of a material by combining cooling experiments in the HTHVESL with specific heat capacity measurements in a DSC. Hence, it was possible to obtain emissivities of deeply undercooled $Zr_{41.2}Ti_{13.8}Cu_{12.5}Ni_{10.0}Be_{22.5}$ liquids down to the glass transition. The hemispherical total emissivity depends linearly on the temperature in the undercooled liquid. In the glass transition region no significant deviations from this behavior are observed, which is due to the fact that the glass transition neither significantly affects the dc resistivity nor the surface morphology of the sample. Furthermore, the specific heat capacity of the whole undercooled liquid region was determined. The results are consistent with the present picture of the temperature dependence of the specific heat capacity in the undercooled liquid.

The authors would like to thank S. Schneider and S. Chung for valuable help and fruitful discussions. This work was supported by the Humboldt Foundation via the Feodor Lynen Program, the Department of Energy (Grant No. DEFG-03-86ER45242) and the National Aeronautics and Space Administration (Grant No. NAG8-954).

[1] P. D. Foote, Bull. Bur. Std. **7**, 607 (1915).
[2] C. Davisson and J. R. Weeks, Jr., J. Opt. Soc. Am. **8**, 581 (1924).
[3] R. Smalley and A. J. Sievers, J. Opt. Soc. Am. **11**, 15 (1978).
[4] A. J. Sievers, J. Opt. Soc. Am. **11**, 1505 (1978).
[5] S. Sasaki, H. Masuda, M. Higano, and N. Hishinuma, Int. J. Thermophys. **15**, 547 (1994).
[6] P. J. Timans, J. Appl. Phys. **74**, 6353 (1993).
[7] A. J. Rulison and W. K. Rhim, Metall. Mater. Trans. B **26**, 503 (1995).
[8] A. Inoue, T. Zhang, and T. Masumoto, Mater. Trans. JIM **31**, 425 (1991).
[9] T. Zhang, A. Inoue, and T. Masumoto, Mater. Trans. JIM **32**, 1005 (1991).
[10] A. Peker and W. L. Johnson, Appl. Phys. Lett. **63**, 2342 (1993).
[11] Y. J. Kim, R. Busch, W. L. Johnson, A. J. Rulison, and W. K. Rhim, Appl. Phys. Lett. **65**, 2136 (1994).
[12] W. K. Rhim, S. K. Chung, D. Barber, K. F. Man, G. Gutt, A. Rulison, and R. E. Spjut, Rev. Sci. Instrum. **64**, 2961 (1993).
[13] R. Busch, Y. J. Kim, and W. L. Johnson, J. Appl. Phys. **77**, 4039 (1995).
[14] A. J. Rulison and W. K. Rhim, Rev. Sci. Instrum. **65**, 695 (1994).
[15] A. H. Okumura, A. Inoue, and T. Masumoto, Acta Metall. Mater. **41**, 915 (1993).
[16] F. Gärtner, Ph.D. thesis, Universität Göttingen, 1992.
[17] R. Busch, F. Gärtner, C. Borchers, P. Haasen, and R. Bormann, Acta Metall. Mater. (to be published).
[18] H. Fecht (private communication).
[19] R. Bormann, F. Gärtner, and K. Zöltzer, Less-Common Metals **145**, 19 (1988).
[20] J. G. Gasser and B. Kefif, Phys. Rev. B **41**, 2776 (1990).
[21] U. Geyer (private communication).
[22] M. La Madrid, Y. J. Kim, and W. L. Johnson, unpublished research, California Institute of Technology, 1995.